Micro-CT Evaluation of Bead Microstructure for Large Area Additive Manufacturing Polymer Composite Deposition

Neshat Sayah

Graduate Research Assistant

Dr. Douglas E. Smith

Professor

(NSF Award No.2055628)

Department of Mechanical Engineering, Baylor University, Waco, Tx

Additive Manufacturing

- Lightweight
- Favorable mechanical properties
- Multifunctional application
- Add details to design with little or no additional costs
- Build a large range of prototypes with complex geometries

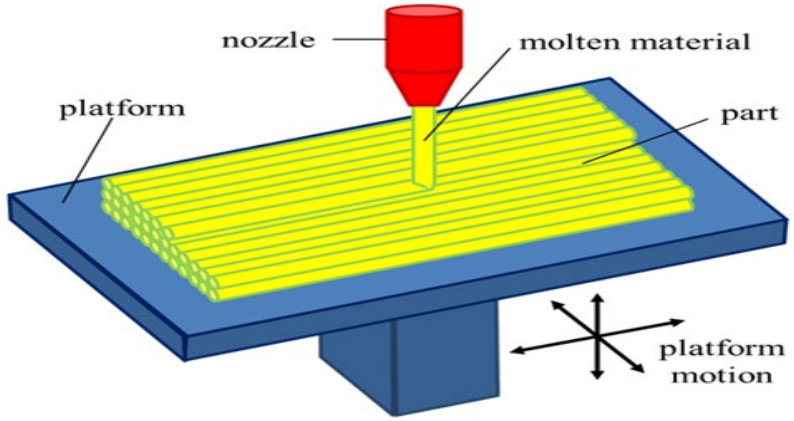

3D Printing Process

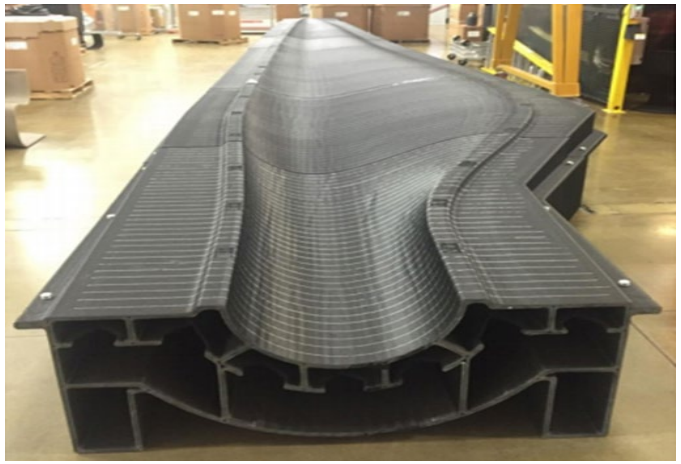

Aerospace trim tool being printed at ORNL's BAAM system – 5.2 m long structure made of ABS with 20% carbon fiber [1].

Shelby Cobra 3D printed car being printed at ORNL's LAAM system [2].

[1] Post, B., Richardson, B., Lloyd, P., Love, L., Nolet, S., and Hannan, J., 2017, *Additive Manufacturing of Wind Turbine Molds*, ORNL/TM--2017/290, CRADA/NFE-16-06051, 1376487.
[2] "Shelby Cobra" [Online]. Available: https://web.ornl.gov/sci/manufacturing/shelby/. [Accessed: 19-Jan-2019].

Composite Materials

Composite material is a material made up of multiple distinct materials that combine to offer a new material with enhanced properties.

- High rigidity
- Good impact resistance
- High dimensional stability
- Good tensile strength

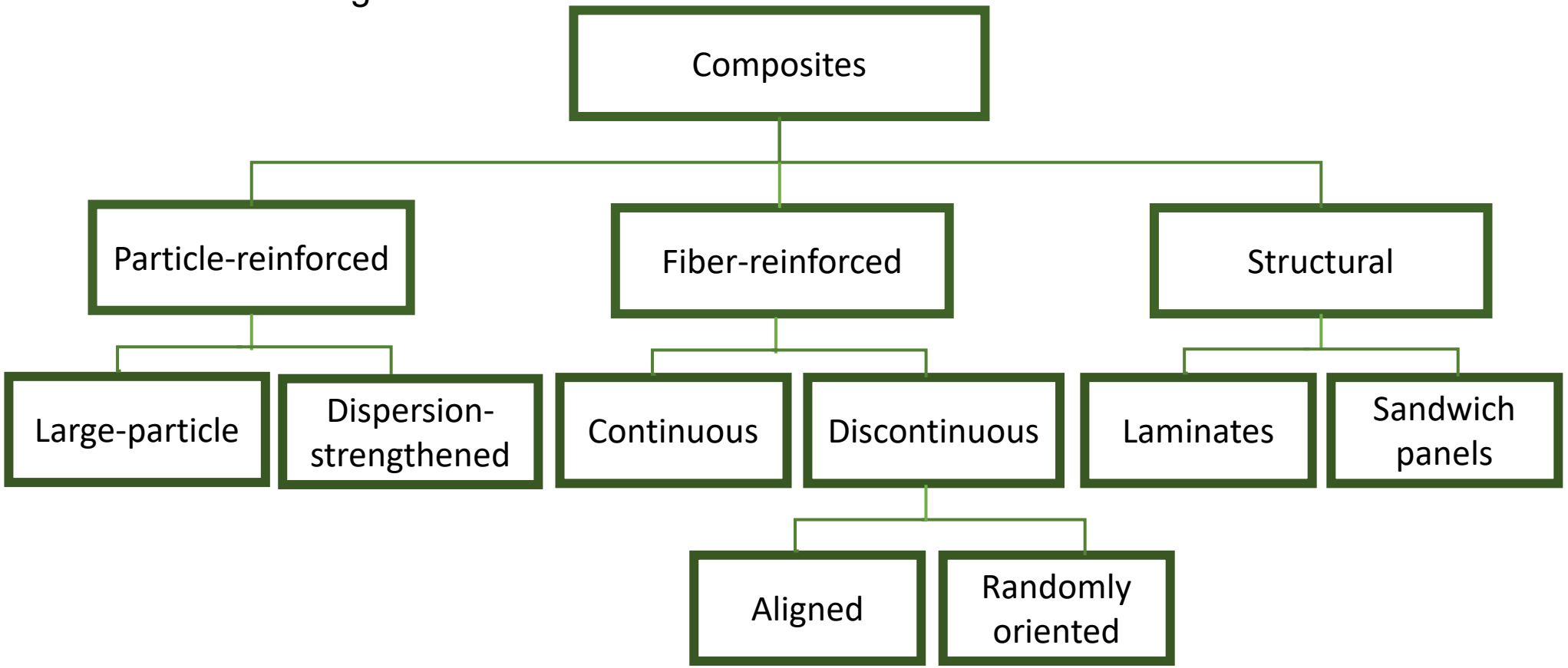

Carbon fiber reinforced polymer composites

Advantages of Carbon Fiber (CF) filled polymers in Polymer deposition AM

- High strength to weight ratio
- Excellent fatigue, corrosion and wear resistance
- Higher modulus (up 4.5X with 13% CF/ABS [4])
- Higher strength (up 3X with 13% CF/ABS [4])
- Increased thermal conductivity
- Improved dimensional stability
- Improved directional properties in bead
- Ability to print in preferred direction

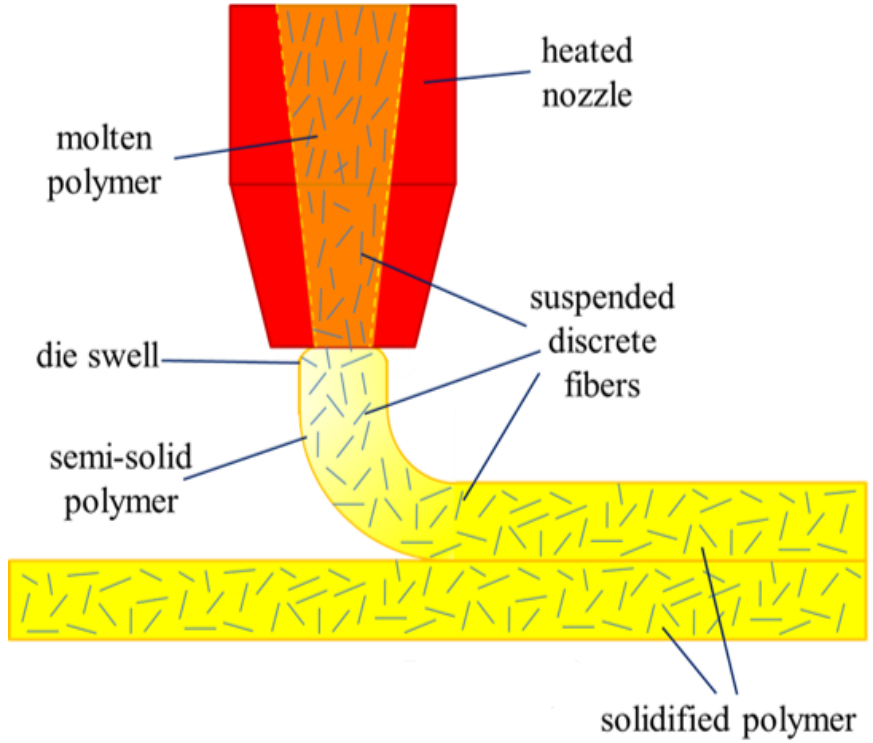

[4] Love, L. J., Kunc, V., Rios, O., Duty, C. E., Elliot, A. M., The Importance of Carbon Fiber to Polymer Additive Manufacturing, *Journal of Materials Research, suppl. Focus Issue: The Materials Science of Additive Manufacturing*, 29(17):1893-1898, 2014.

Fiber Orientation

Fiber Orientation Tensor

Fiber orientation is calculated using orientation tensors [7]

$$\frac{DA}{Dt} = -\frac{1}{2}(\Omega \cdot A - A \cdot \Omega) + \frac{1}{2}\lambda(\Gamma \cdot A + A \cdot \Gamma - 2\mathbb{A}:\Gamma) + D_r$$

Where:

$A_{ij} = \oint p_i p_j \psi(\mathrm{p}) dS$ (2nd order fiber orientation tensor)

$A_{ij} = A_{ji}$

$A_{ijkl} = \oint p_i p_j p_k p_l \psi(\mathrm{p}) dS$ (4th order fiber orientation tensor)

$A_{ijkl} = A_{jikl} = A_{ijlk} = A_{kjil} = A_{ljki} = A_{ilkj}$

$A_{ijkk} = A_{ji}$

ψ = the probability density function for fiber orientation

D_r= Rotary Diffusion Function

$$\begin{pmatrix} p_1 = \sin\theta\cos\varphi \\ p_2 = \sin\theta\sin\varphi \\ p_3 = \cos\theta \end{pmatrix}$$

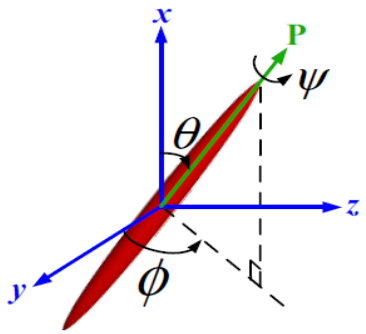

Orientation of a single rigid fiber

Random Orientation

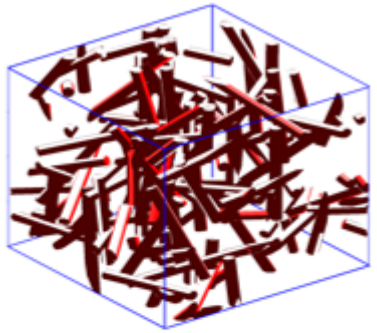

$$A_{ij} = \begin{bmatrix} 1/3 & 0 & 0 \\ 0 & 1/3 & 0 \\ 0 & 0 & 1/3 \end{bmatrix}$$

Uniaxial Alignment

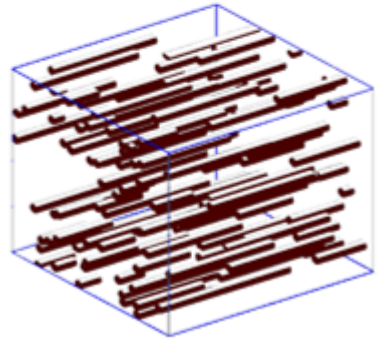

$$A_{ij} = \begin{bmatrix} 1 & 0 & 0 \\ 0 & 0 & 0 \\ 0 & 0 & 0 \end{bmatrix}$$

[5].Kugler, S.K., Kech, A., Cruz, C. and Osswald, T., 2020. Fiber orientation predictions—a review of existing models. *Journal of Composites Science*, *4*(2), p.69.

[6]. Cintra Jr, J.S. and Tucker III, C.L., 1995. Orthotropic closure approximations for flow-induced fiber orientation. *Journal of Rheology*, *39*(6), pp.1095-1122.

[7]. Advani, S.G. and Tucker III, C.L., 1987. The use of tensors to describe and predict fiber orientation in short fiber composites. *Journal of rheology*, *31*(8), pp.751-784.

Microstructural Voids

Why Study Voids?

- Voids significantly impact the physical and thermomechanical properties
- Voids decrease interlaminar shear strength and longitudinal compressive strength
- Void decreases tensile modulus

Factors Influencing Void Formation

- Adding carbon fiber changes the polymer rheology and therefore increase the void volume fraction
- Air entrapment in flow process during processing stages
- Difference in the matrix-fiber coefficient of thermal expansion
- Differential cooling rate between the external surface and core regions
- Voids nucleation occurs at fiber ends

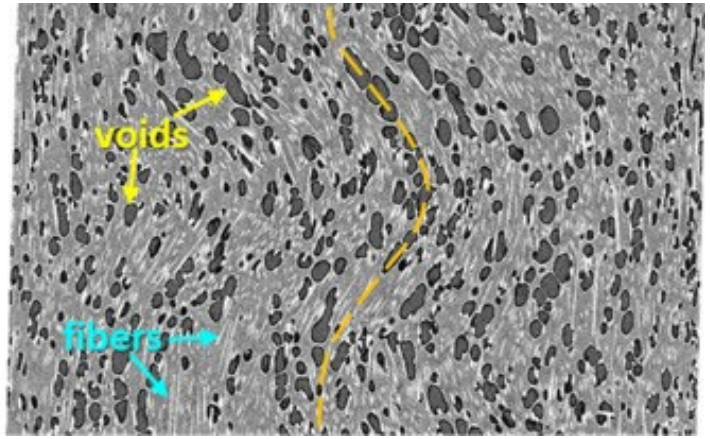

2D view of voids and carbon fibers in 3D printed carbon fiber/ PEEK using X-ray computed tomography[9].

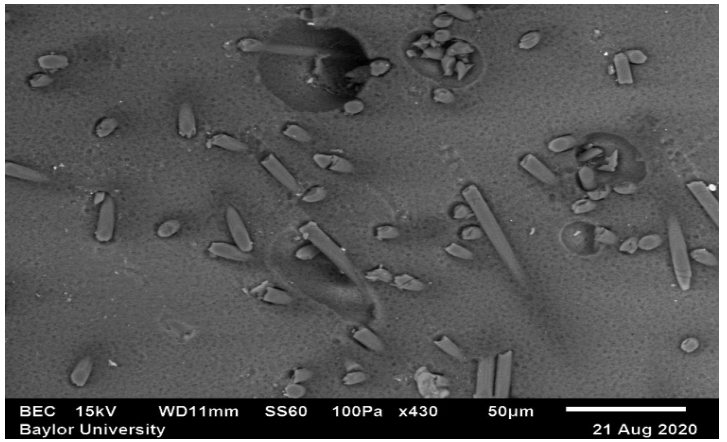

SEM image of CF/ABS [10].

[8] Vaxman, A., Narkis, M., Siegmann, A. and Kenig, S., 1989. Void formation in short-fiber thermoplastic composites. Polymer composites, 10(6), pp.449-453.

[9] Sommacal, S., Matschinski, A., Drechsler, K. and Compston, P., 2021. Characterisation of void and fiber distribution in 3D printed carbon-fiber/PEEK using X-ray computed tomography. *Composites Part A: Applied Science and Manufacturing*, *149*, p.106487.

[10] Nargis, R.A., 2021. Internal fiber orientation measurements and void distribution for large area additive manufactured parts using optical and SEM imaging techniques.

Void characterization techniques

Density determination

- Destructive
- Void volume fraction information
- Inaccurate No information about void shape and size

$$Vv = 100 - \rho_c^m \left(\frac{W_r}{\rho_r} + \frac{W_f}{\rho_f} \right)$$

Resin wight percentage

Fiber wight percentage

Void content

Measured composite density

Resin density

Fiber density

Microscopy

Scanning Electron Microscope (SEM)

- Non-destructive
- Section-bias error
- Location-bias error
- Void volume fraction information
- 2D details of void shape and size information

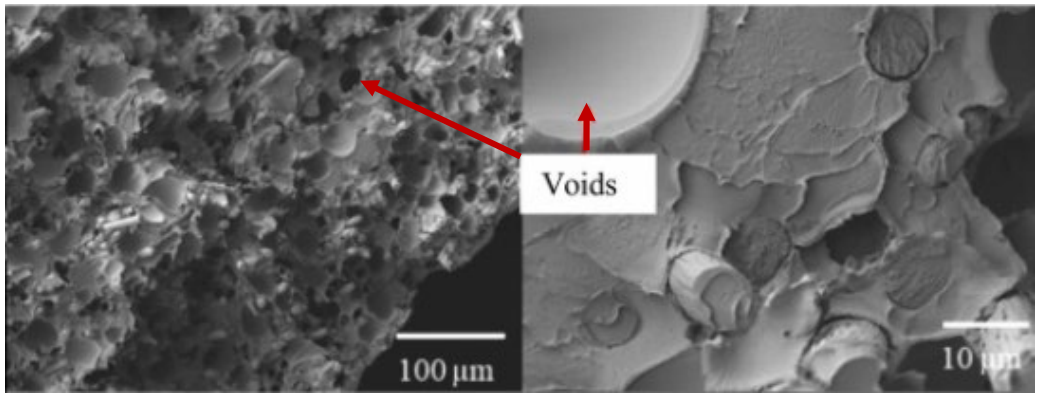

SEM images of 30 wt% CF-PEEK/PEI [11]

X-ray micro–Computed Tomography

- Non-destructive
- Void volume fraction information
- 3D details of void shape, size and distribution

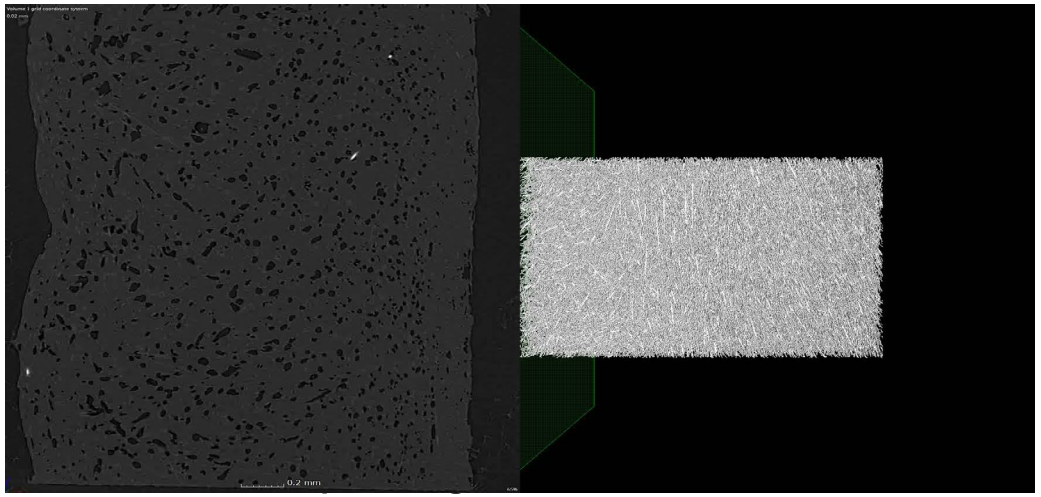

[11]. Diouf-Lewis, A., Farahani, R.D., Iervolino, F., Pierre, J., Abderrafai, Y., Lévesque, M., Piccirelli, N. and Therriault, D., 2022. Design and characterization of carbon fiber-reinforced PEEK/PEI blends for Fused Filament Fabrication additive manufacturing. Materials Today Communications, 31, p.103445.

Experimental Evaluation of Microstructural Properties

Baylor's LAAM system

Printing parameter	Value
Temperature	210 °C
Nozzle Height	1.5 mm
Roller Height	1.35 mm
Screw Speed	2250 rpm
Nozzle Diameter	3.172 mm

3D printing parameters

13 wt % Carbon fiber reinforced ABS
3D printed using LAAM system

NSI X3000 micro-CT system [10].

Parameter	Value
Voltage	60 (kV)
Current	350 (µA)
Resolution	10(µm)
Time	75 (Minutes)

NSI X3000 micro-CT scan parameters

VOLUME GRAPHICS

[10]. https://commons.wikimedia.org/wiki/File:Volume-Graphics_logo.svg

Samples in this study

- 13 (wt%) Carbon fiber reinforced acrylonitrile butadiene styrene (CF/ABS) pellets purchased from PolyOne
- Single CF/ABS strand extruded in the air
- Regular CF/ABS bead
- Roller-Printed CF/ABS bead

Printing parameter	Value
Temperature	210 °C
Nozzle Height	1.5 mm
Roller Height	1.35 mm
Screw Speed	2250 rpm
Nozzle Diameter	3.172 mm

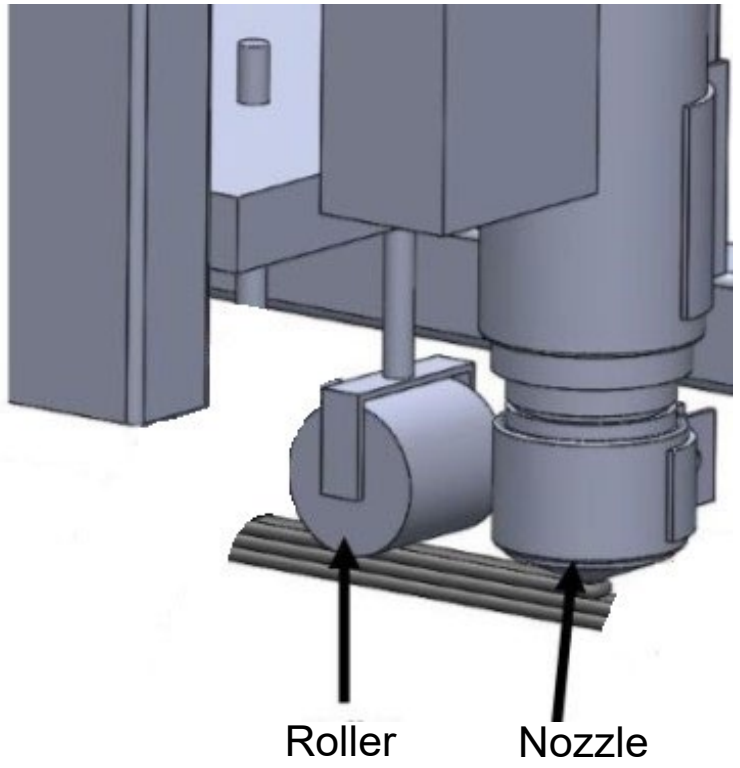

Schematic of printed bead using roller

Study outcomes

- Void volume fraction and distribution
- Directional dependence of void volume fraction
- Void's shape and sphericity
- Void's sphericity variation

Void volume fraction along the coordinate directions of CF/ABS pellet

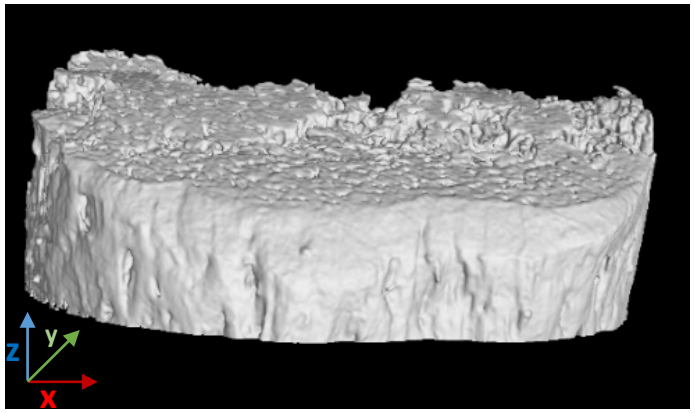

µCT 3D view of scanned pellet

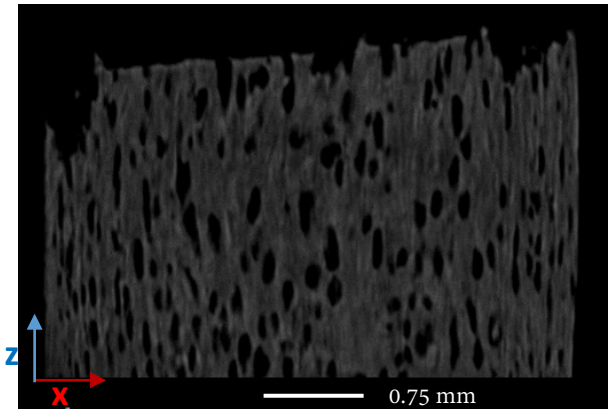

µCT 2D front view (x-z plane) of pellet

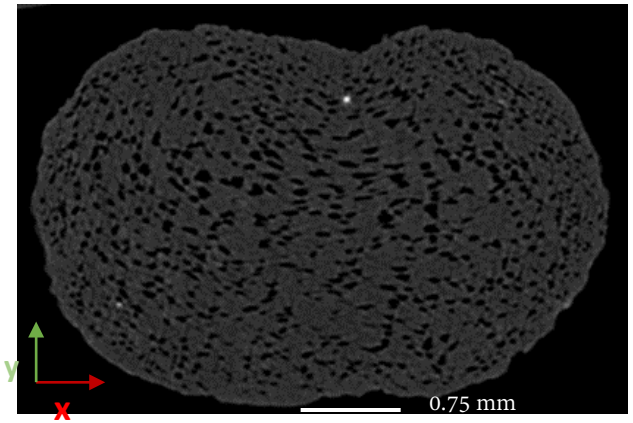

µCT 2D top view (x-y plane) of pellet

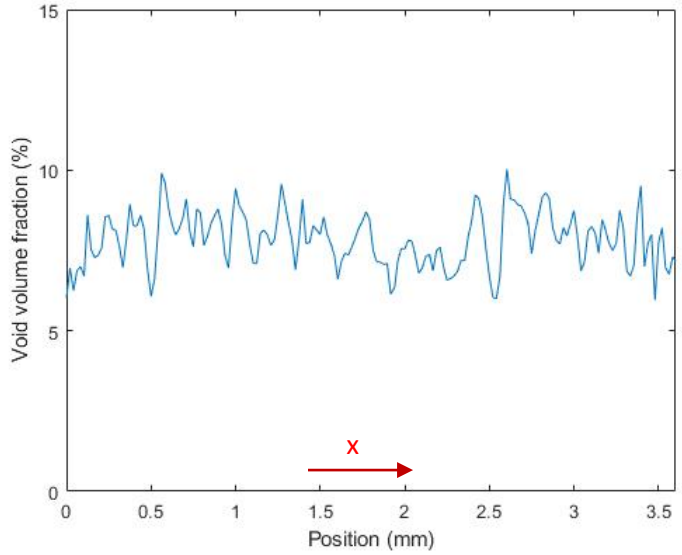

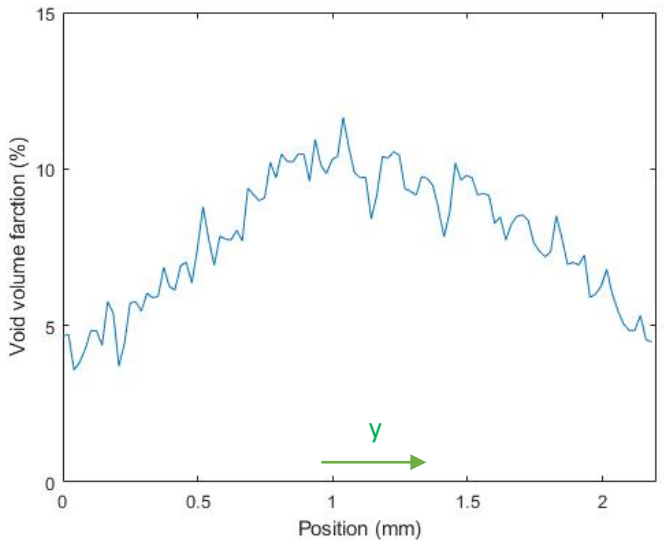

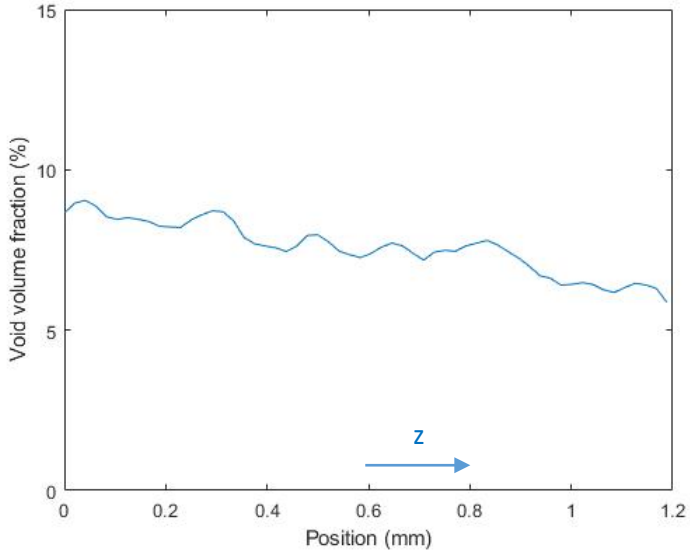

Void volume fraction along the coordinate directions of CF/ABS pellet

- Void volume fraction is 7.78% within the pellet
  - Voids elongated in the extrusion direction (z direction)
  - Void volume fraction has the highest amount in the center of pellet

Void volume fraction along the coordinate directions of single CF/ABS strand extruded in the air

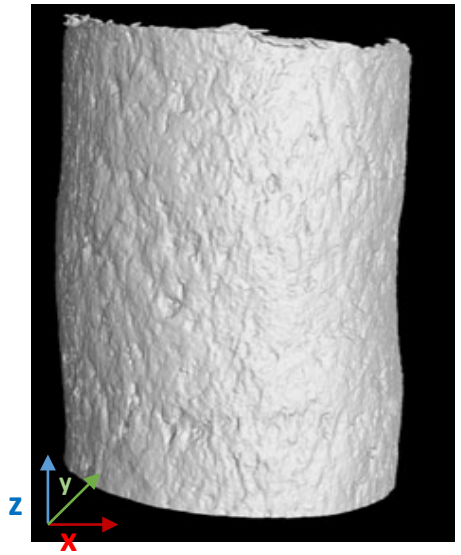

µCT 3D view of scanned strand

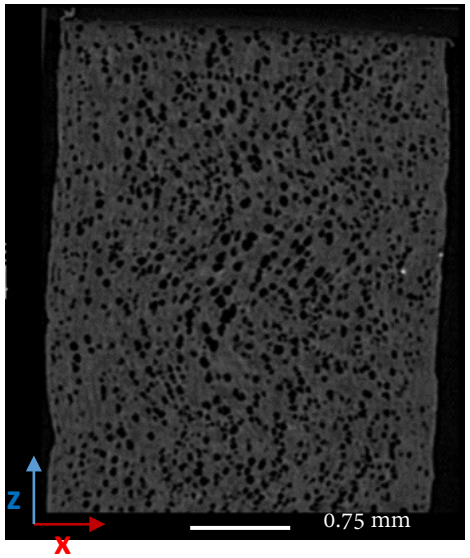

µCT 2D front view (x-z plane) of strand

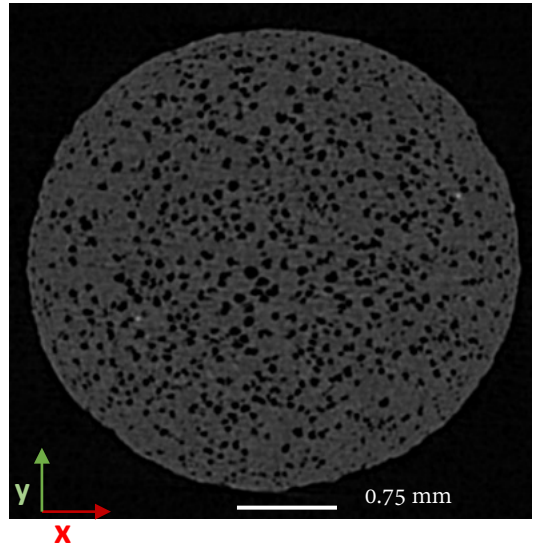

µCT 2D top view (x-y plane) of strand

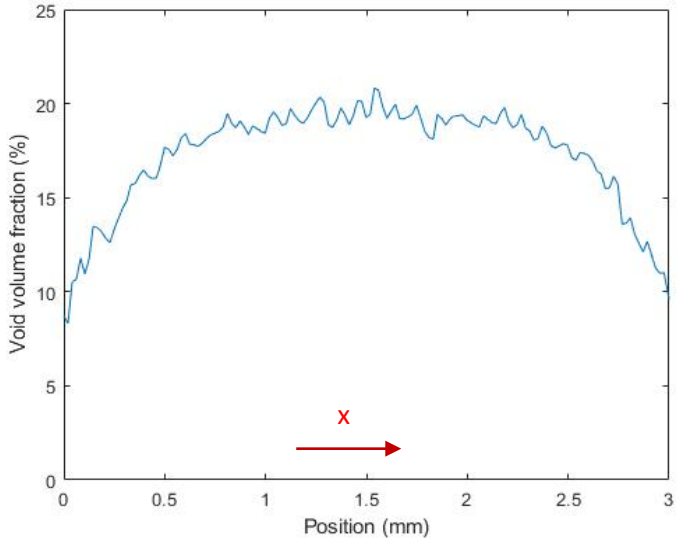

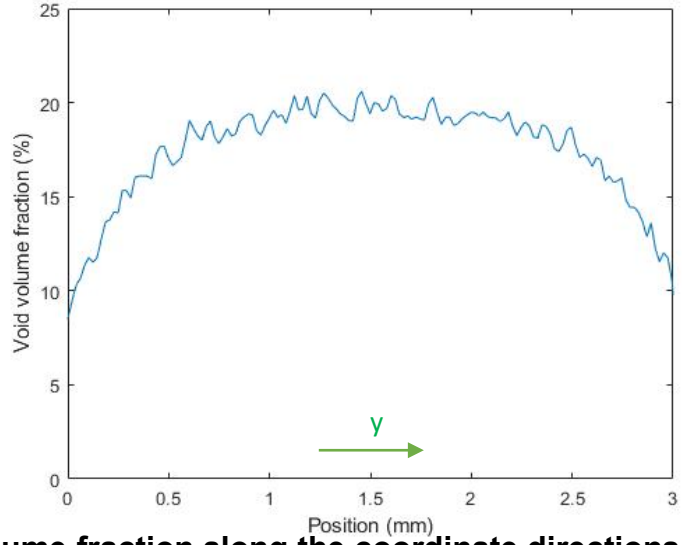

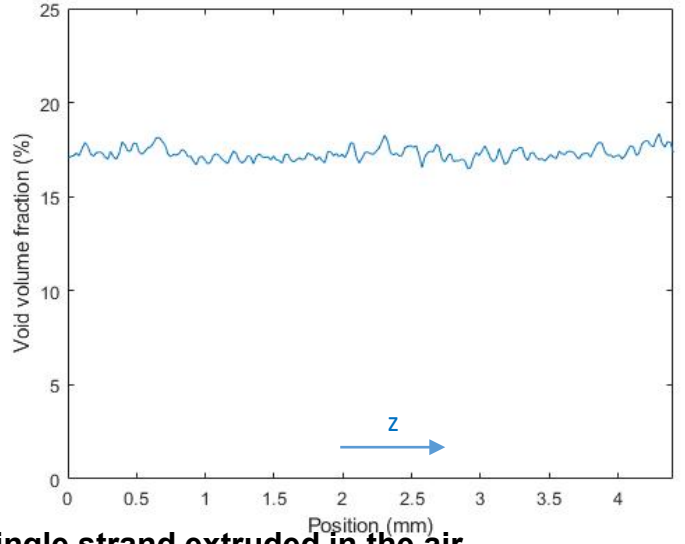

Void volume fraction along the coordinate directions of single strand extruded in the air

- Void Volume fraction significantly increases from 7.78% in the pellet to 17.2% in the strand due to the extrusion process
  - Void volume fraction has the highest amount in the center of the strand
  - Void volume fraction is uniform along the extrusion direction

Void volume fraction along the coordinate directions of the regular CF/ABS bead

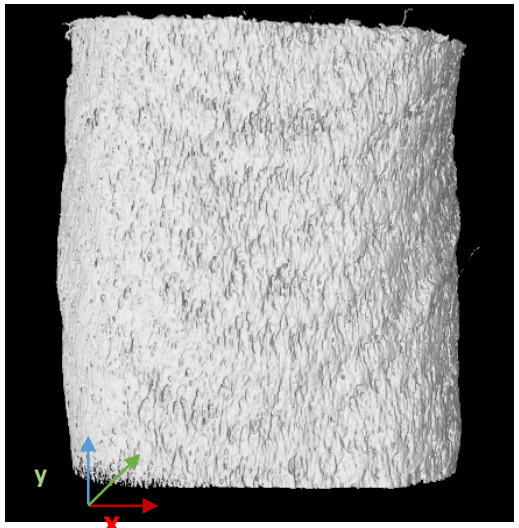

µCT 3D view of scanned regular bead

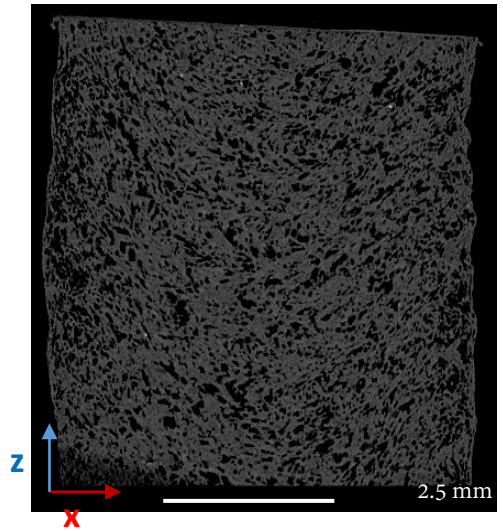

µCT 2D front view (x-z plane) of regular bead

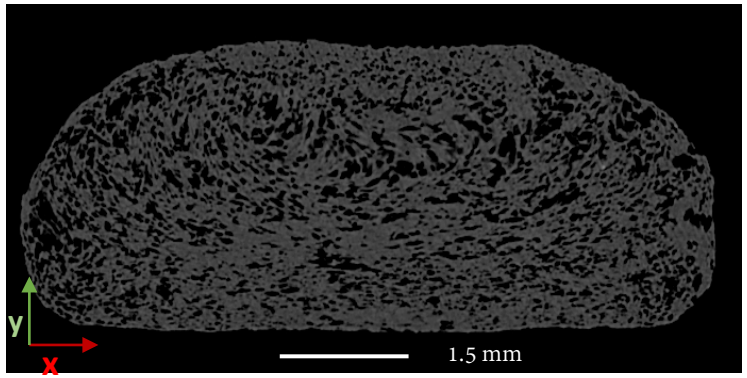

µCT 2D top view (x-y plane) of regular bead

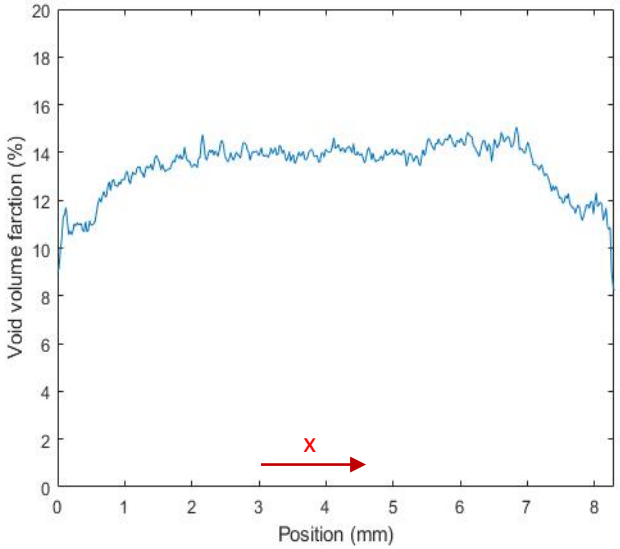

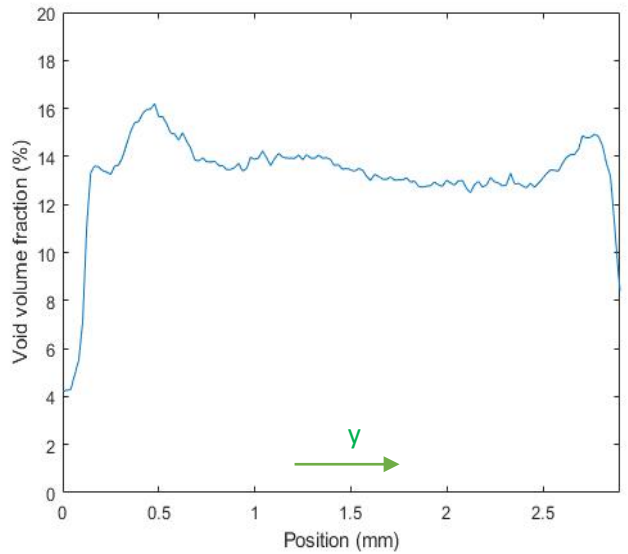

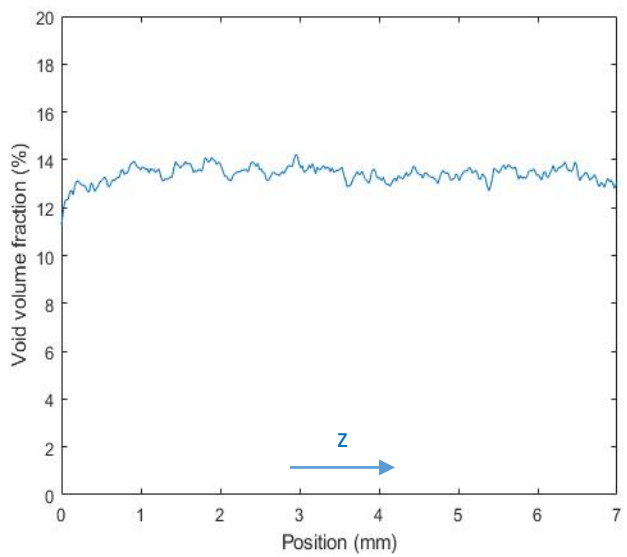

Void volume fraction along the coordinate directions of the regular bead

- Void volume fraction reduces from 17.2% in the strand to 13.56% in the regular bead due to the deposition on the bed
  - Void volume fraction is uniform along the extrusion direction
  - Void volume fraction is lower near the edges

Void volume fraction along the coordinate directions of the roller-printed CF/ABS bead

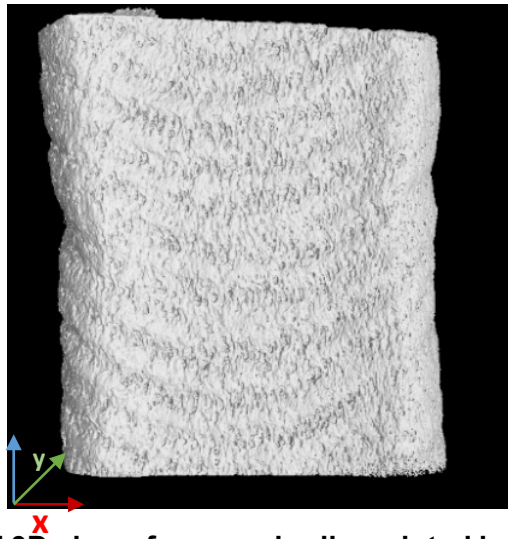

µCT 3D view of scanned roller printed bead

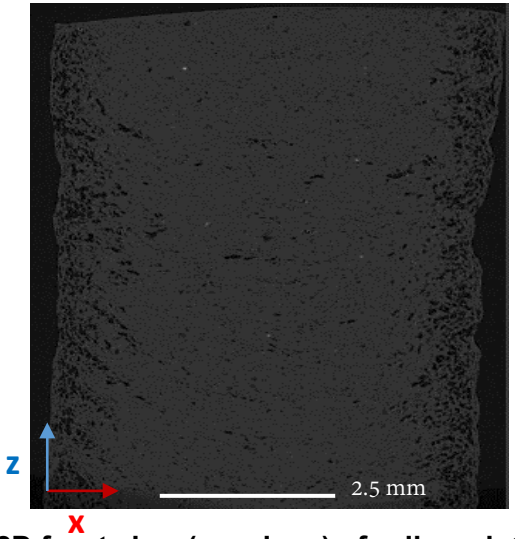

µCT 2D front view (x-z plane) of roller printed bead

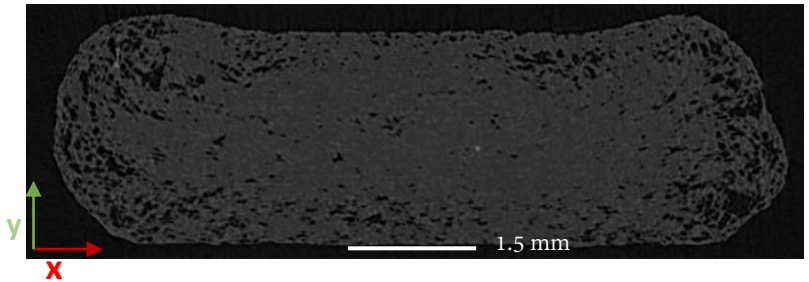

µCT 2D top view (x-y plane) of roller printed bead

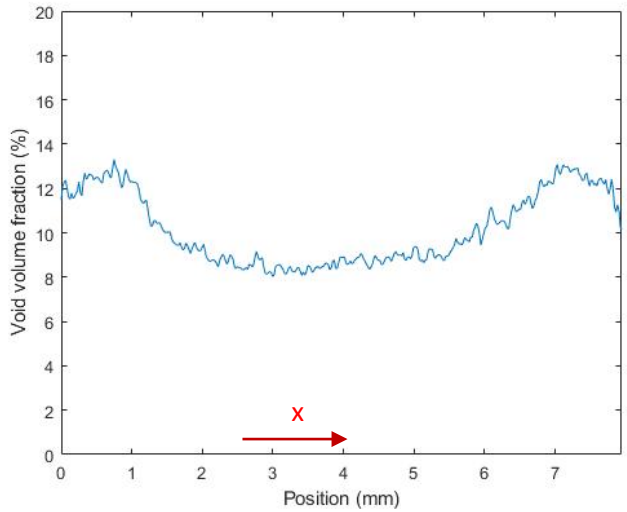

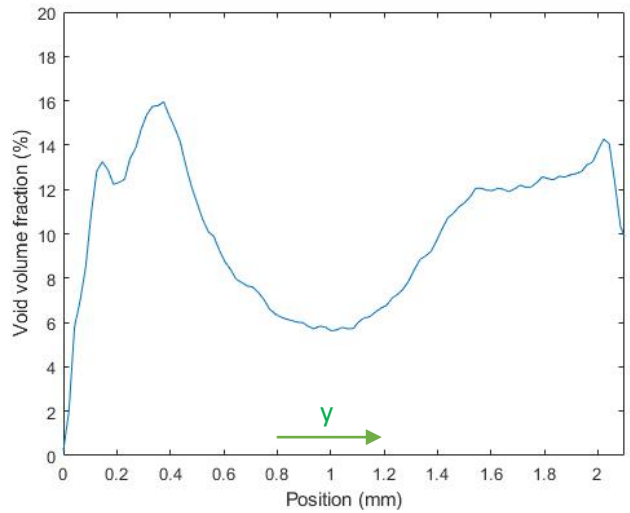

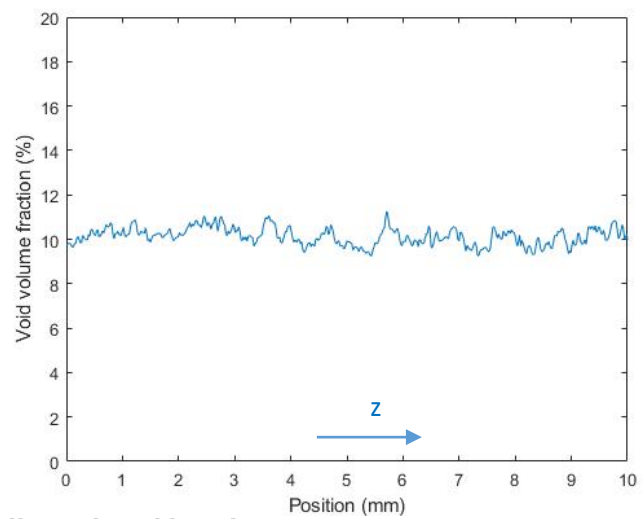

Void volume fraction along the coordinate directions of the roller-printed bead

- Using roller during the printing process reduces void volume fraction from 13.56% in regular bead to 10.12%
  - Void volume fraction is uniform along the extrusion direction
  - Unlike regular bead, void volume fraction is higher near the edges than the center of the roller printed bead

Void sphericity

Void sphericity defined as the ratio between the surface area of a sphere with the same volume as a single void and the surface area of the detected void.

$$\text{Sphericity} = \frac{A_{sphere}}{A_{void}}$$

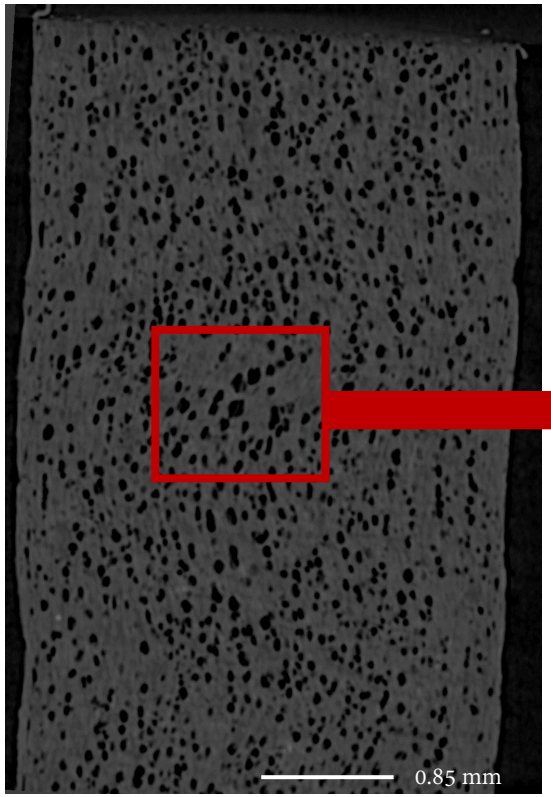

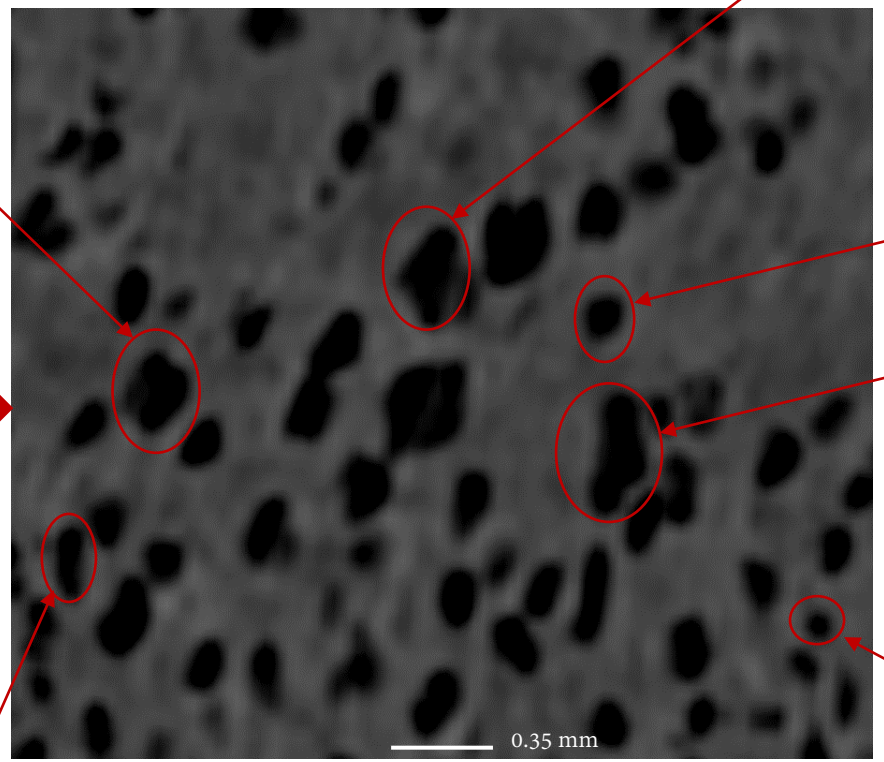

Sphericity of 0.45

Sphericity of 0.31

Sphericity of 0.72

Sphericity of 0.31

Sphericity of 0.79

Sphericity of 0.36

Void sphericity

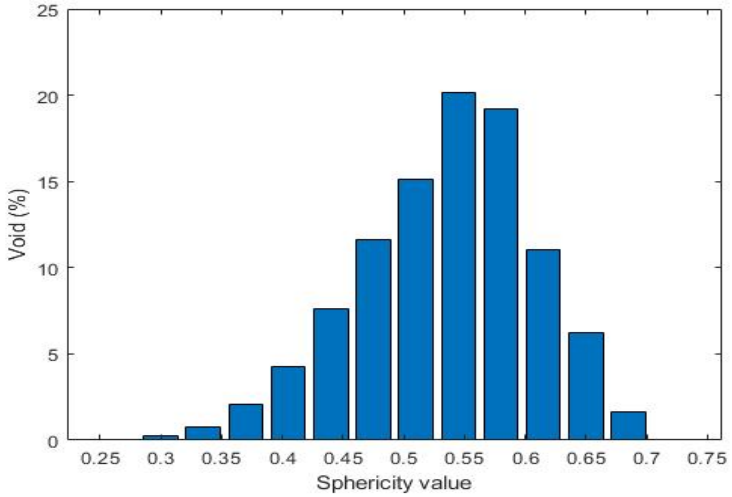

(a)

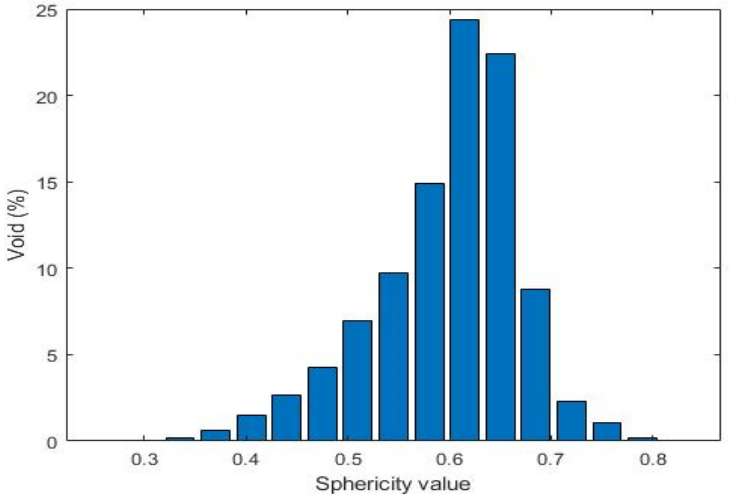

(b)

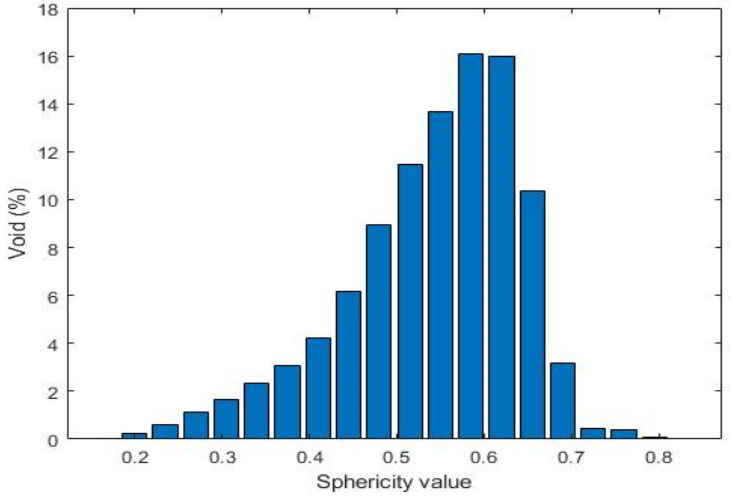

(c)

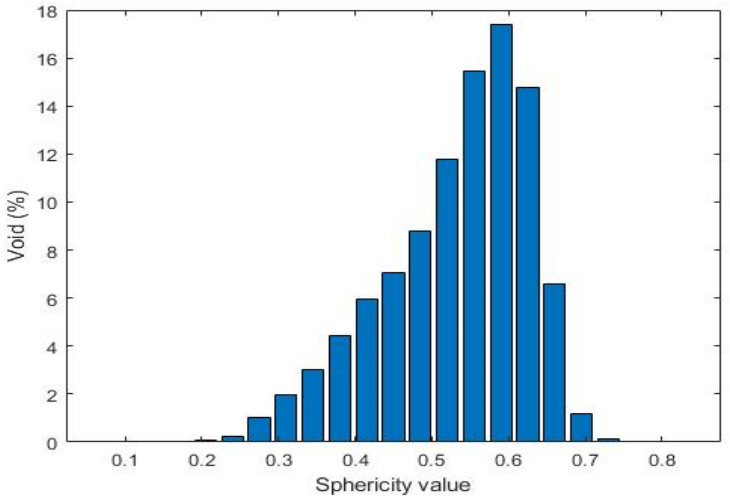

(d)

Void sphericity within a) CF/ABS pellet b) single strand c) regular bead, d) roller-printed bead

Void sphericity

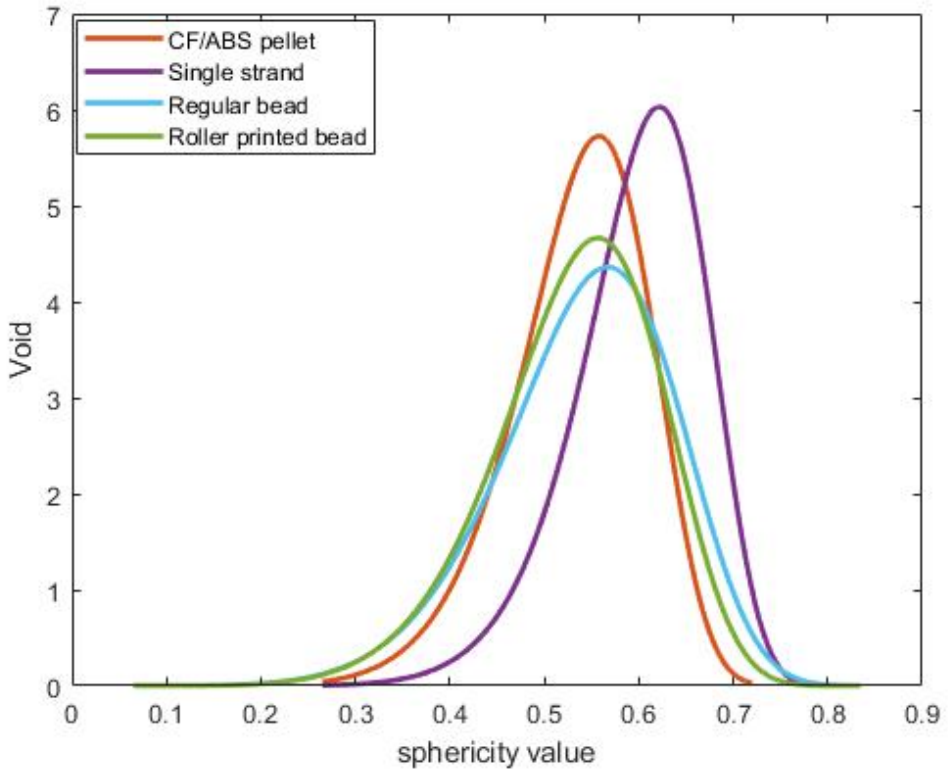

Weibull distribution of void sphericity in different scanned parts

Sample	Scale parameter	Shape parameter	Skewness
CF/ABS pellet	0.60	9.10	-0.30
Single strand	0.62	10.24	-0.33
Regular bead	0.58	6.80	-0.25
Roller printed bead	0.56	7.13	-0.26

- Void are more in sphere shape within the microstructure of the single strand than the pellet.
- Void sphericity is lower within the microstructure of the roller printed bead compared to regular bead.

Effect of printing process parameters on void volume fraction within the microstructure regular CF/ABS bead

Temperature (°C)	Extrusion rate (rpm)	Nozzle height (mm)
200-205-210	1750	1
210-215-220	2000	1.1
220-225-230	2250	1.2

Printing process parameters

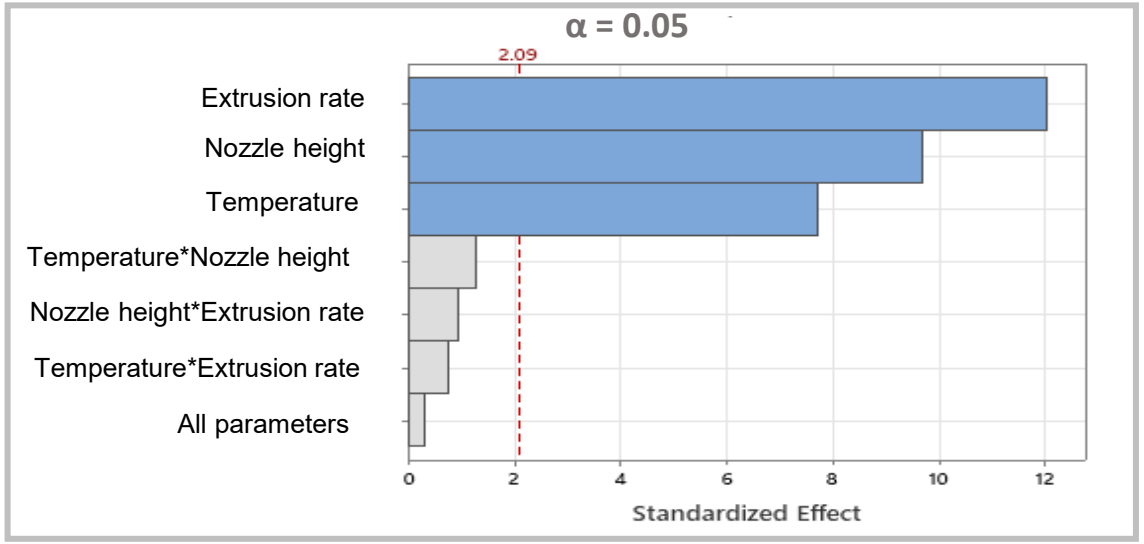

Pareto Chart of the standardized effects of printing parameters on void volume fraction

Among all three printing process parameters in this study, extrusion rate has the highest effect on void volume fraction while temperature has the lowest impact.

Effect of printing process parameters on void volume fraction within the microstructure regular CF/ABS bead

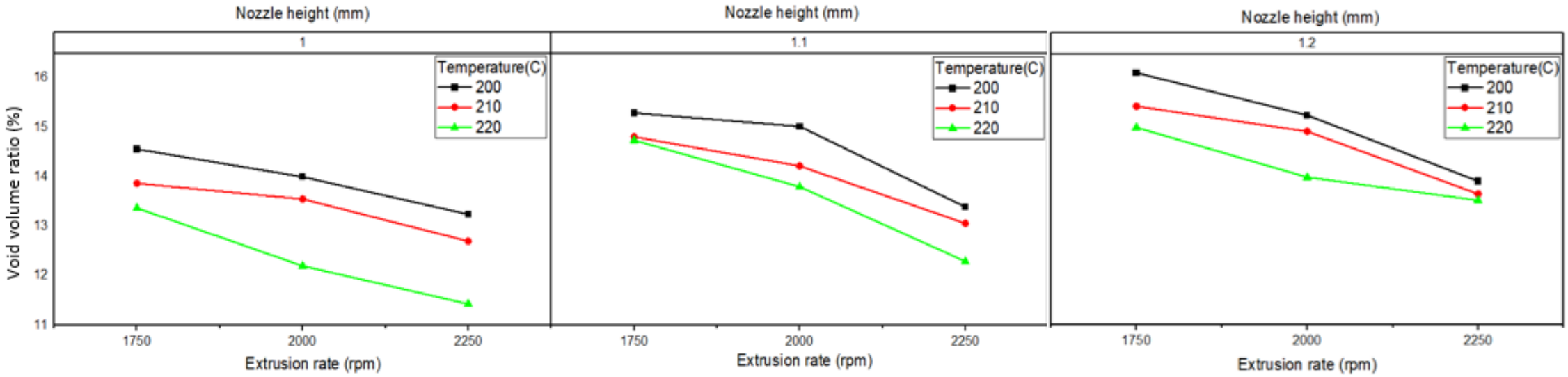

Effect of printing process parameters on void volume fraction

- Void volume fraction decreases by increasing the extrusion rate from 1750 rpm to 2250 rpm.
- Void volume fraction decreases by increasing temperature from 200°C to 220°C.
- Void volume fraction increases by increasing the nozzle height above the printing bed.

Conclusion

Void volume fraction

- Voids existed in the microstructure of the pellet which explains the printing process is not the only factor that causes voids formation within the microstructure of the 3D printed parts.
- Void volume fraction reduces during the deposition of bead on print bed
- Using a roller during the printing process significantly reduces the void volume fraction.

Void sphericity

- Among all four scanned parts, voids within the pellet have the lowest sphericity ranges (more irregular shapes), and voids within the single strand have the highest sphericity ranges (more sphere shapes).

Effect of printing process parameters on void volume fraction

- Void volume fraction decreases by increasing the extrusion rate from 1750 rpm to 2250 rpm and temperature from 200°C to 220°C.
- Void volume fraction increases by increasing the nozzle height above the printing bed.

Future work and Acknowledgment

- Develop a relationship between print processing parameters and carbon fiber orientation, length and volume fraction within the microstructure of beads.
- Effect of print process parameters on void's shape and size within the microstructure of beads.
- Thanks to NSF for awarding this research project (NSF Award No. 2055628).
- Thanks to L3Harris company for funding this project.
- Thanks to Dr. Russell and Dr. Kokkada for their help on LAAM and μCT systems.

References

[1] Post, B., Richardson, B., Lloyd, P., Love, L., Nolet, S., and Hannan, J., 2017, *Additive Manufacturing of Wind Turbine Molds*, ORNL/TM--2017/290, CRADA/NFE-16-06051, 1376487.

[2] “Shelby Cobra” [Online]. Available: https://web.ornl.gov/sci/manufacturing/shelby/. [Accessed: 19-Jan-2019].

[3] Love, L. J., Kunc, V., Rios, O., Duty, C. E., Elliot, A. M., The Importance of Carbon Fiber to Polymer Additive Manufacturing, *Journal of Materials Research, suppl. Focus Issue: The Materials Science of Additive Manufacturing*, 29(17):1893-1898, 2014.

[4]Kugler, S.K., Kech, A., Cruz, C. and Osswald, T., 2020. Fiber orientation predictions—a review of existing models. *Journal of Composites Science*, *4*(2), p.69.

[5] Cintra Jr, J.S. and Tucker III, C.L., 1995. Orthotropic closure approximations for flow-induced fiber orientation. *Journal of Rheology*, *39*(6), pp.1095-1122.

[6] Advani, S.G. and Tucker III, C.L., 1987. The use of tensors to describe and predict fiber orientation in short fiber composites. *Journal of rheology*, *31*(8), pp.751-784.

[8] Vaxman, A., Narkis, M., Siegmann, A. and Kenig, S., 1989. Void formation in short-fiber thermoplastic composites. Polymer composites, 10(6), pp.449-453.

[9] Sommacal, S., Matschinski, A., Drechsler, K. and Compston, P., 2021. Characterisation of void and fiber distribution in 3D printed carbon-fiber/PEEK using X-ray computed tomography. *Composites Part A: Applied Science and Manufacturing*, *149*, p.106487.

Thank you